Mammalian *Exo1* encodes both structural and catalytic functions that play distinct roles in essential biological processes

Sonja Schaetzlein[a,1], Richard Chahwan[a,1], Elena Avdievich[a], Sergio Roa[a,b], Kaichun Wei[c], Robert L. Eoff[d], Rani S. Sellers[e], Alan B. Clark[f,g], Thomas A. Kunkel[f,g], Matthew D. Scharff[a,2], and Winfried Edelmann[a,2]

Departments of [a]Cell Biology and [e]Pathology, Albert Einstein College of Medicine, Bronx, NY 10461; [b]Oncology Division, Center for Applied Medical Research, University of Navarra, 31008 Pamplona, Spain; [c]Department of Obstetrics and Gynecology, University of Missouri, Kansas City, MO 64108; [d]Department of Biochemistry and Molecular Biology, University of Arkansas for Medical Sciences, Little Rock, AR 72205; and [f]Laboratory of Molecular Genetics and [g]Laboratory of Structural Biology, National Institute of Environmental Health Sciences, National Institutes of Health, Research Triangle Park, NC 27709

Contributed by Matthew D. Scharff, May 9, 2013 (sent for review January 3, 2013)

Mammalian Exonuclease 1 (EXO1) is an evolutionarily conserved, multifunctional exonuclease involved in DNA damage repair, replication, immunoglobulin diversity, meiosis, and telomere maintenance. It has been assumed that EXO1 participates in these processes primarily through its exonuclease activity, but recent studies also suggest that EXO1 has a structural function in the assembly of higher-order protein complexes. To dissect the enzymatic and nonenzymatic roles of EXO1 in the different biological processes in vivo, we generated an EXO1-E109K knockin (*Exo1*^{EK}) mouse expressing a stable exonuclease-deficient protein and, for comparison, a fully EXO1-deficient (*Exo1*^{null}) mouse. In contrast to *Exo1*$^{null/null}$ mice, *Exo1*$^{EK/EK}$ mice retained mismatch repair activity and displayed normal class switch recombination and meiosis. However, both *Exo1*-mutant lines showed defects in DNA damage response including DNA double-strand break repair (DSBR) through DNA end resection, chromosomal stability, and tumor suppression, indicating that the enzymatic function is required for those processes. On a transformation-related protein 53 (*Trp53*)-null background, the DSBR defect caused by the E109K mutation altered the tumor spectrum but did not affect the overall survival as compared with *p53-Exo1*^{null} mice, whose defects in both DSBR and mismatch repair also compromised survival. The separation of these functions demonstrates the differential requirement for the structural function and nuclease activity of mammalian EXO1 in distinct DNA repair processes and tumorigenesis in vivo.

somatic hypermutation | scaffold function | ssDNA

Exonuclease 1 (EXO1) belongs to the XPG/Rad2 family of metallonucleases and was first described as a 5′–3′ exonuclease associated with meiosis in *Schizosaccharomyces pombe* (1). Since then EXO1 has been implicated in a multitude of eukaryotic DNA metabolic pathways and in maintaining genomic integrity. It is involved in DNA mismatch repair (MMR) by hydrolyzing DNA mismatches (2–4), in DNA double-strand break repair (DSBR) through DNA end resection (5–7), in B-cell development through the generation of antibody diversity (8), and in telomere maintenance by promotion of telomeric recombination (9). Biochemical analysis had shown that the N-terminal half of EXO1 possesses 5′–3′ exonuclease and 5′ flap-endonuclease activities (10). However, these apparently distinct functions now are thought to be mechanistically unified (11).

MMR is essential for maintaining the integrity of eukaryotic genomes by removing misincorporated nucleotides that result from erroneous replication. During MMR, the repair of distinct types of mismatches is initiated by two partially redundant MutS homolog (MSH) complexes: the MSH2–MSH6 (MutSα) heterodimer, that recognizes and binds to single-base mispairs and single-base insertion/deletions, and the MSH2–MSH3 (MutSβ) complex that primarily interacts with single-base and larger insertions/deletions. Subsequent to mismatch recognition by the MSH complexes, a MutL homolog (MLH) complex consisting of MLH1-PMS2 (MutLα) is recruited to activate subsequent repair events in an ATP-dependent manner (12–14). In addition, genetic studies indicate that a second MutL complex consisting of MLH1–MLH3 (MutLγ) plays a role in the repair of a proportion of insertion/deletion mutations (15, 16). EXO1 interacts with MutSα and MutLα both in yeast and humans (2, 17). Biochemical analysis attributed a role for EXO1 in the 5′- and 3′-directed excision of the nascent mismatch-containing DNA strand downstream of MMR protein recruitment (3, 4). It has been assumed that excision by EXO1 is dependent on its nuclease activity despite the lack of clear in vivo evidence. On the other hand, studies in yeast suggested a nuclease-independent function for EXO1 as an adapter or structural scaffold in the formation of MMR protein complexes (18–20).

MMR proteins facilitate the immune response because they participate in an error-prone process that promotes the affinity maturation of antibodies by increasing somatic hypermutation (SHM) at Activation-induced deaminase (AID)–induced U:G mismatches at the Ig locus (21). Conversely, defects in MMR can lead to increased mutation rates elsewhere in the genome and are associated with hereditary nonpolyposis colorectal cancer (HNPCC or Lynch syndrome) and 15–25% of sporadic colorectal cancers (CRCs) in humans (22–24). Because of the involvement of EXO1 in MMR, it was speculated that *EXO1* mutations might

Significance

Exonuclease1 (EXO1) is involved in a variety of DNA repair pathways and is implicated in multiple biological processes. To determine the contribution of the enzymatic and structural functions of EXO1 in these processes, we compared mice with catalytically inactive EXO1-knockin and complete EXO1-knockout mutations. We found that the catalytic function of EXO1 is essential for the DNA damage response, double-strand break repair, chromosomal stability, and tumor suppression, whereas EXO1's structural role alone is critical for mismatch repair, antibody diversification, and meiosis. Our study reveals differential requirements for both EXO1 functions in DNA repair and tumorigenesis in vivo.

Author contributions: S.S., R.C., E.A., S.R., T.A.K., M.D.S., and W.E. designed research; S.S., R.C., E.A., S.R., K.W., R.L.E., and A.B.C. performed research; S.S., R.C., S.R., K.W., R.L.E., R.S.S., M.D.S., and W.E. analyzed data; and S.S., R.C., M.D.S., and W.E. wrote the paper.

The authors declare no conflict of interest.

Freely available online through the PNAS open access option.

[1]S.S. and R.C. contributed equally to this work.

[2]To whom correspondence may be addressed. E-mail: matthew.scharff@einstein.yu.edu or winfried.edelmann@einstein.yu.edu.

This article contains supporting information online at www.pnas.org/lookup/suppl/doi:10.1073/pnas.1308512110/-/DCSupplemental.

contribute to HNPCC or CRC. However, the role of EXO1 in suppressing CRC remains unclear despite *EXO1* germ-line mutations being found in patients with atypical HNPCC (25, 26).

Like DNA mismatches, double-strand breaks (DSBs) are a form of genotoxic lesions. An early response to DSBs is 5′–3′ DNA end resection, which generates ssDNA that evokes the checkpoint and homologous recombination (HR) responses. Although the identity of DNA helicases and nucleases that process DSBs are not yet as well defined in humans as in yeast (5, 6), studies from both species suggest a two-step model for DNA DSB processing. MRE11-RAD50-NBS1 (MRN) and CtIP initiate the end-trimming of the DSB, which is followed by the generation of longer stretches of ssDNA by either EXO1 or the Bloom syndrome protein (BLM)–DNA2 helicase–nuclease complex (5, 27). Deficiencies in DSBR lead to chromosomal instability, infertility, neurodegeneration, tumorigenesis, premature aging, and a decrease in class switching in the immune system that requires nonhomologous end joining (NHEJ) (28). However, the way in which EXO1 is involved in all these processes remains unclear.

Previous yeast studies suggest both exonuclease-dependent and -independent functions for EXO1 in MMR and meiosis (18, 29), but the implications of distinct EXO1 functions in these biological processes remain ambiguous. We therefore generated and analyzed two mouse lines to assess the role of the structural and enzymatic functions in vivo. One line carries a HNPCC-modeled *E109K* knockin mutation in the exonuclease domain of EXO1 (termed $Exo1^{EK}$). The other line carries an *Exo1*-null knockout mutation leading to the complete loss of EXO1 protein expression (termed $Exo1^{null}$).

Results

Generation of $Exo1^{null}$ and Nuclease-Deficient $Exo1^{E109K}$ Mice. We previously generated *Exo1*-mutant mice ($Exo1^{\Delta 6}$) that express normal levels but a truncated form of EXO1 lacking exon 6 (4). Because exon 6 encodes the interface region spanning both the nuclease and structural domains of EXO1, we could not clearly attribute the phenotypes we observed to either function. A better separation-of-function mutation was needed to address those issues. Because EXO1-E109 is evolutionarily conserved from yeast to humans (Fig. 1*A*), we decided to model the E109K mutation (termed $Exo1^{EK}$) found in HNPCC patients in mice. Our decision to use this mutation also was based on previous biochemical studies showing that the E109K mutation leads to abrogation of the exonucleolytic activity of human EXO1 (30). This mutation does not affect protein stability, DNA binding, or protein interactions (Fig. 1*B* and Fig. S1) (25, 30). For comparison, and to eliminate any possibility of structural function that might occur in the exon 6-deficient mice, we also generated a complete *Exo1*-knockout mouse line (termed $Exo1^{null}$) that does not express any EXO1 protein (Fig. 1*C* and Fig. S1*E*). RT-PCR, cDNA-sequencing, and Northern Blot analyses verified expression of the mutant allele in $Exo1^{EK}$ mice and loss of *Exo1* mRNA in $Exo1^{null}$ mice (Fig. S1). The stable expression of WT and mutant $EXO1^{E109K}$ protein and the loss of EXO1 were verified by Western blot analysis (Fig. S1*E*). The biochemical analysis of the exonuclease domains of recombinant EXO1 and $EXO1^{E109K}$ showed impaired enzymatic activity of the mutant mammalian protein (Fig. S2 and Table S1) commensurate to the lack of activity observed in the yeast *exo1-D173A* mutant, which is considered the canonical nuclease-dead *Exo1* mutant (31).

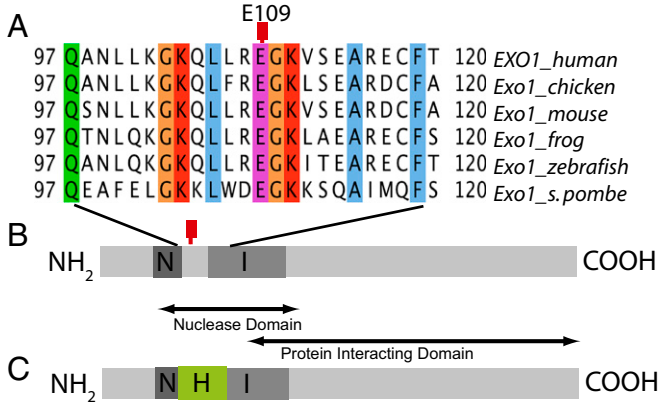

Fig. 1. Generation of *Exo1*-mutant mice. (*A*) Amino acid alignment of the EXO1 protein. Note that EXO1-E109 (red rectangle) and the surrounding amino acids are conserved from yeast to human. (*B*) Functional motifs of EXO1 and the location of the EXO1-E109K knockin mutation (red rectangle) identified in atypical HNPCC. N-terminal (N) and internal (I) RAD2 domains are indicated. (*C*) Location of the Hygromycin cassette (H) disrupting exons 4 and 5 in the *Exo1*-null mutation. See also Fig. S1.

Structural Function of EXO1 Is Required for in Vivo MMR. To investigate the effect of the null and EK mutations on MMR, we determined the genomic mutation rates at the *cII* reporter locus in several tissues of 12-wk-old $Exo1^{EK/EK}$, $Exo1^{null/null}$, and WT littermates. In DNA isolated from spleen, liver, and small intestine, mutation frequencies were significantly increased in $Exo1^{null/null}$ mice as compared with WT mice (Fig. 2*A*). Surprisingly, $Exo1^{EK/EK}$ mice did not show an increase in mutation frequency in any of the tissues analyzed (Fig. 2*A*). The analysis of mutation spectra revealed that the majority of mutations comprised transition mutations and, to a lesser extent, transversions (Table 1). However, $Exo1^{null/null}$ mice displayed a two- to three-fold increase in mutation frequency and an increase in transversions (Table 1) in the analyzed organs as compared with either $Exo1^{+/+}$ or $Exo1^{EK/EK}$ mice (Fig. 2*A*).

Nuclease Function Is Required for MMR-Mediated DNA Damage Response Signaling via ssDNA. In addition to repairing replication errors, MMR also plays a critical role in the cellular response to many DNA-damaging agents (32–34). MMR-proficient cells respond to cisplatin, 6-thioguanine (6-TG), and nucleophilic substitution 1 (S_N1) DNA methylators such as methylnitronitrosoguanidine (MNNG) by undergoing G_2 arrest followed by apoptosis. The MMR-dependent activation of the G_2 checkpoint and apoptosis are thought to be caused by the creation of ssDNA that leads to DSB resulting from futile attempts by the MMR pathway to repair damaged bases in the parental DNA strand (futile cycle model) (35). In addition, MMR complexes were suggested to function as DNA damage sensors that activate the DNA damage-signaling network (direct signaling model) (36, 37). To determine the role of Exo1 in the MMR-mediated DNA Damage Response (DDR) signaling, we exposed $Exo1^{+/+}$, $Exo1^{EK/EK}$, and $Exo1^{null/null}$ immortalized mouse embryonic fibroblasts (MEFs) to MNNG. These studies showed that both the complete loss of EXO1 in $Exo1^{null/null}$ cells and of the nuclease function in $Exo1^{EK/EK}$ cells lead to increased resistance to MNNG (Fig. 2*B*). In addition, we found that the MNNG-dependent formation of ssDNA gaps and DSBs as assessed by phosphorylation of replication protein A (RPA) and gamma histone 2AX (γH2AX), respectively, was reduced in both $Exo1^{null/null}$ and $Exo1^{EK/EK}$ cells (Fig. 2 *C* and *D*). These results indicate that the nuclease function of EXO1 facilitates the formation of ssDNA gaps during MMR-mediated DDR signaling, as is consistent with the futile cycle model.

Structural Function of EXO1 Is Required for SHM. Enzymatically mediated U:G mismatches produced by AID in B cells are considered a physiological form of regulated mismatch-based mutations and participate in the production of higher-affinity antibodies through SHM. EXO1 is required to introduce mutations at A:T base pairs of Ig Variable (V) regions (8). Current

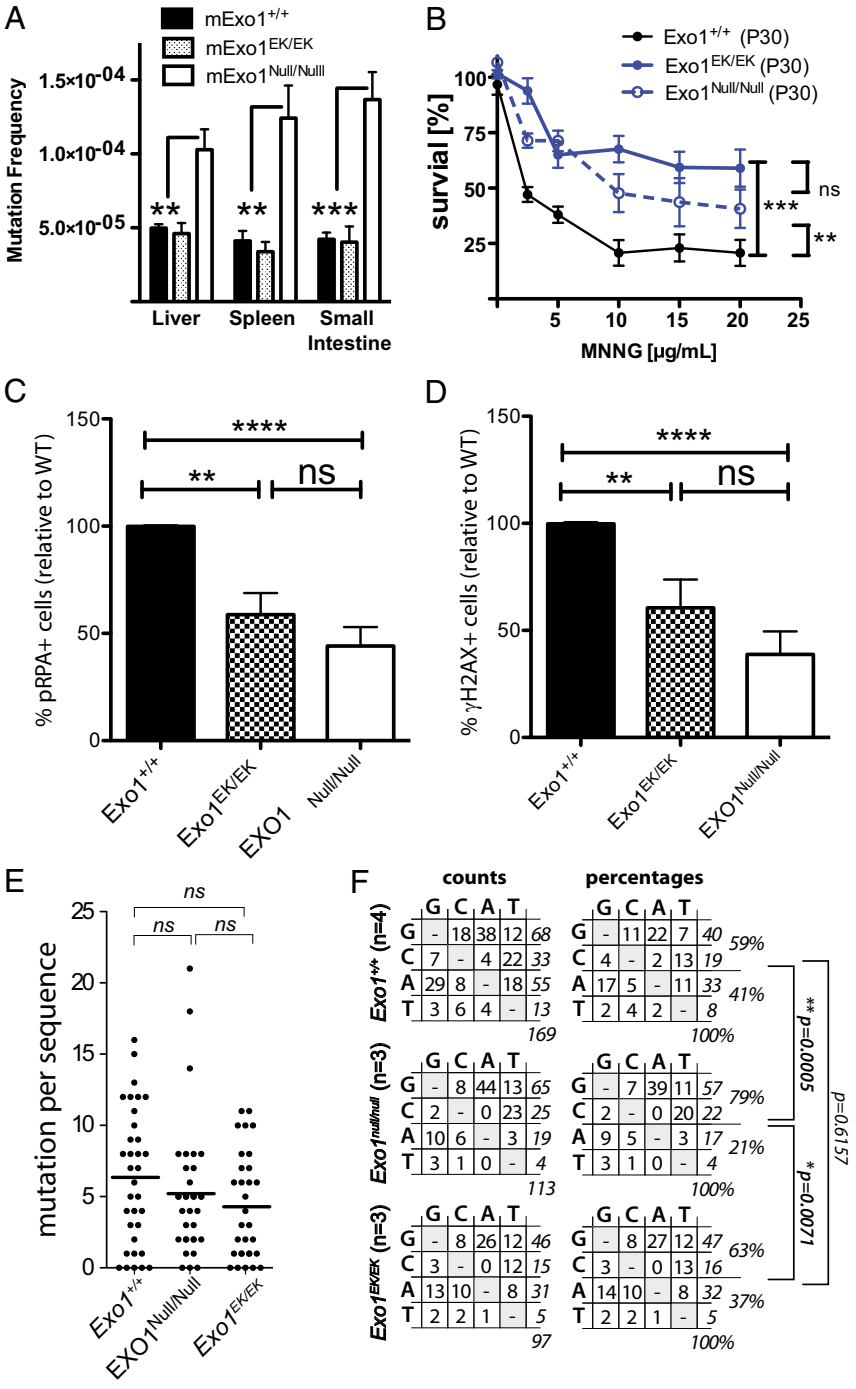

Fig. 2. Exonuclease activity is not required for MMR and SHM. (*A*) *cII* reporter gene mutation frequencies in spleen, liver, and small intestine of 12-wk-old WT, *Exo1*$^{EK/EK}$, and *Exo1*$^{null/null}$ mice (n = 5 mice for each genotype). Data represent mean ± SD. A total of 271 mutations were sequenced for WT mice, 245 for *Exo1*$^{EK/EK}$ mice, and 371 for *Exo1*$^{null/null}$ mice. Note that mutation frequency is increased by two- to threefold in *Exo1*$^{null/null}$ mice as compared with *Exo1*$^{EK/EK}$ mice and WT controls. (*B*) Cell survival of immortalized MEFs of the indicated genotypes after MNNG treatment. (*C*) Histogram of the rates of RPA2-pS4/S8–positive cells in MNNG-treated MEFs of the indicated genotypes. (*D*) Histogram of the rates γH2AX-positive cells in MNNG-treated MEFs of the indicated genotypes. Data represent mean ± SEM. (*E*) Number of mutations in each of the V186.2 sequences that were cloned and analyzed per genotype. Black horizontal bars indicate the mean. (*F*) Chart showing the spectrum of mutations within the V186.2 V region for NP-immunized mice. When the cumulative percentages of G:C and A:T mutations pooled from all animals within the three cohorts are compared, only *Exo1*$^{null/null}$ mice exhibited a decrease in A:T and increase in G:C mutations as compared with WT or *Exo1*$^{EK/EK}$ mice. No significant changes in SHM were detectable in *Exo1*$^{EK/EK}$ mice compared with WT littermates. The two-tailed probabilities associated with the resulting z-ratio for the significance of the difference between two independent proportions were calculated as shown at right. ns, not significant. **P < 0.01; ***P < 0.001; ****P < 0.0001.

models suggest that EXO1-dependent resection of the area surrounding U:G mismatches and the recruitment of error-prone polymerases contribute to SHM (38, 39). To test whether the nuclease activity of the EXO1 protein is directly required for SHM, we examined *Exo1*-mutant and WT mice for their phenotype with regard to the error-prone repair of Ig V regions. The

Table 1. In vivo mutation spectra at the *cII* reporter locus in *Exo1*$^{null/null}$, *Exo1*$^{EK/EK}$, and *Exo1*$^{+/+}$ littermates

	Exo1$^{+/+}$ (%)	*Exo1*$^{EK/EK}$ (%)	*Exo1*$^{null/null}$ (%)
Mutated sequences	271 (100)	245 (100)	371 (100)
Transversions	34 (13)	42 (17)	93 (25)*
Transitions	222 (82)	189 (77)	269 (73)
Insertion/deletions	15 (6)	14 (6)	9 (2)

*Increased mutation frequency significantly different compared with *Exo1*$^{+/+}$ and *Exo1*$^{EK/EK}$.

SHM process, in response to NP-CGG immunization, was measured by examining the accumulation of mutations in splenic B cells at the heavy chain V186.2 region. Although there was a trend toward a decrease in the overall mutation frequency of the mutant mice (WT 5.2×10^{-2}, null 4.6×10^{-2}, EK 3.9×10^{-2}), with the decrease in EK mice just achieving statistical significance, the average number of mutations per sequence was not significantly different among the WT, *Exo1*$^{null/null}$, and *Exo1*$^{EK/EK}$ groups (Fig. 2*E*). When the spectra of mutations were analyzed, only *Exo1*$^{null/null}$ mice exhibited a statistically significant decrease in the frequency of mutations at A:T base pairs in Polymerase eta (Polη) hotspots (41% versus 21%) and a bias toward transition mutations at G:C base pairs (59% and 79%) (Fig. 2*F*) compared with WT, which was not observed in the *Exo1*$^{EK/EK}$ group. Combined with the above data, this result suggests that EXO1 nuclease activity, but not its structural scaffold, is largely dispensable for both the correction of replication errors during MMR and the generation of mutations at A:T bases at the Ig V regions during SHM in vivo.

EXO1 Nuclease Activity Is Required for the Repair of DNA DSBs Through DNA End Resection. DNA DSBs are extremely cytotoxic and can be generated by exogenous agents (e.g., ionizing radiation) or endogenous processes, either destructive (e.g., stalled replication fork collapse) or constructive [e.g., meiotic recombination and class switch recombination (CSR)]. Failure to repair these lesions can cause, among other defects, gross chromosomal aberrations that are intimately implicated in carcinogenesis (40). To investigate the role of EXO1 in DSBR, we examined metaphases of *Exo1*$^{EK/EK}$, *Exo1*$^{null/null}$, and WT MEFs for chromosomal breaks. A comparable increase in the number of such chromosomal breaks was observed in both *Exo1*$^{EK/EK}$ and *Exo1*$^{null/null}$ MEFs as compared with WT, indicating that the enzymatic function of EXO1 is required for effective DSB repair (Fig. 3 *A* and *B*).

To examine the mechanistic role of EXO1 in DSB resection and signaling, we exposed WT, *Exo1*$^{EK/EK}$, and *Exo1*$^{null/null}$ primary MEFs to camptothecin (CPT), which induces DSBs specifically in S-phase, and counted the number of RPA foci. After binding to ssDNA, RPA is hyperphosphorylated (pRPA) by DNA damage-responsive protein kinases, such as ataxia telangiectasia mutated (ATM) and ataxia telangiectasia mutated and Rad3 related (ATR). To avoid nonspecific staining, only pRPA foci cells that also were γH2AX positive were counted. Both *Exo1*- mutant cell lines showed significantly reduced colocalization of activated pRPA-S4/S8 and γH2AX, indicating impaired DSB resection in response to CPT treatment (Fig. 3 *C* and *D*). This result suggests an indispensable role for the enzymatic activity of EXO1 in DSB resection. To determine whether the lack of adequate ssDNA generation observed in EXO1 nuclease-deficient cells bears any gross cellular phenotype, we conducted cell-survival experiments. WT, *Exo1*$^{EK/EK}$, and *Exo1*$^{null/null}$ genetically immortalized MEFs were treated with CPT, and surviving colonies were counted 7 d later. The survival of both *Exo1*-mutant MEFs was compromised as compared with WT (Fig. 3*E*), further showing that EXO1 nuclease activity is required for effective DSBR.

Nuclease Activity Is Dispensable for the Role of EXO1 in the Instigation and NHEJ Processing of DSBs During CSR. Like meiosis in germ cells, CSR in B cells requires the regulated generation of DSBs at the switch regions at the Ig locus. Although these DSBs are known to be resolved by classical NHEJ rather than HR, a significant subset of CSR also occurs via a microhomology-mediated alternative NHEJ (41, 42). Microhomology requires limited DNA end resection, and CtIP and EXO1 are likely candidates to contribute to this process. Because CtIP recently has been shown to affect the outcome of CSR (43), we wanted to examine the effects of the loss of EXO1 or its nuclease activity on CSR. Consistent with *Exo1*$^{\Delta 6/\Delta 6}$ studies (8), in *Exo1*$^{null/null}$ mice stimulations with LPS or LPS and IL-4 failed to induce efficient CSR from IgM to IgG3 or to IgG1, respectively (Fig. 4*A*). This failure was not caused by impaired cell proliferation (Fig. 4*B*). Mutant *Exo1*$^{EK/EK}$ B cells, however, did not show a substantial defect in their ability to switch to either isotype compared with WT cells. These data suggest that, although the EXO1 protein is essential during CSR, its nuclease activity is not involved in the early steps of CSR by promoting the generation of the AID- and MMR-triggered DSBs at the switch regions, nor does it

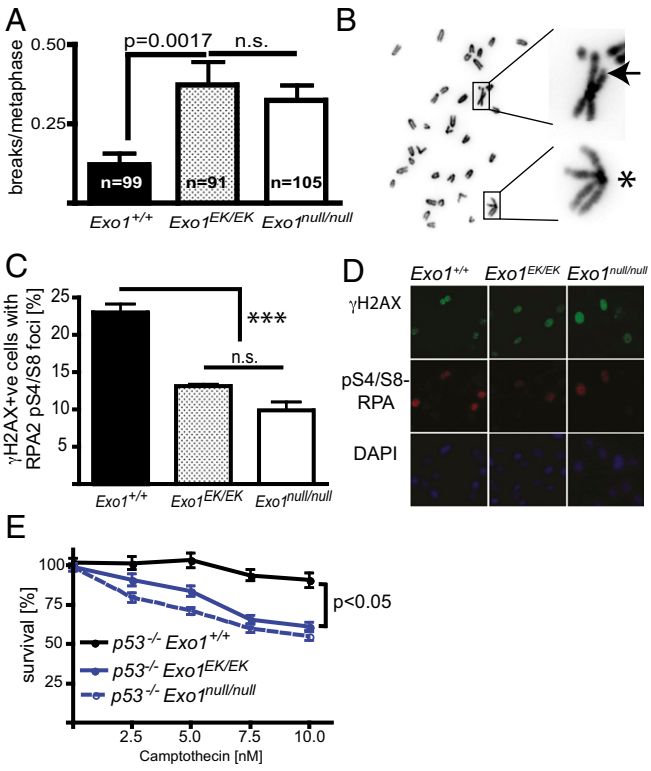

Fig. 3. Exonucleolytic activity of EXO1 is required for DSBR and chromosomal stability in MEFs. (*A*) Histogram of the observed frequency of chromosomal breaks in primary MEFs (passage 3) of the indicated genotypes. Data represent mean ± SD. (*B*) Representative photographs showing breaks (arrow) and fusions (asterisk) in MEF metaphases. (Magnification: 1,000×.) A total of 99 WT, 92 *Exo1*$^{EK/EK}$, and 105 *Exo1*$^{null/null}$ metaphases in four different cell lines per genotype were examined. (*C*) Histogram of the rates of γH2AX-positive cells with RPA2-pS4/S8 foci in MEFs of the indicated genotypes. n.s., not significant; ***$P < 0.001$. (*D*) Representative photographs showing γH2AX- (*Top*), pS4/S8-RPA2- (*Middle*), and DAPI- (*Bottom*) stained MEF after camptothecin treatment (1 h, 1 μM) of the indicated genotypes. (Magnification: 1,000×.) (*E*) Cell survival of immortalized MEFs of the indicated genotypes after CPT treatment. Data present mean ± SD.

participate in the later steps of DNA end processing once the DSB ensues.

Structural Function of EXO1 Is Required for Meiosis. *Exo1*$^{null/null}$ mice of both sexes were sterile. Strikingly, both *Exo1*$^{EK/EK}$ males and females were fertile, suggesting normal meiotic progression. The testis size of *Exo1*$^{EK/EK}$ mice was similar to that of WT littermates, whereas the testis size *Exo1*$^{null/null}$ mice was reduced (Fig. 5 *A* and *B*), and this reduction was not caused by decreased body weight of adult males (Fig. 5*C*). The analysis of spermatogenesis in *Exo1*$^{null/null}$ mice showed that only a very small number of spermatogenic cells progressed through to meiosis II, as indicated by the very few spermatozoa that could be retrieved from the epididymis of *Exo1*$^{null/null}$ adult males (Fig. 5*D*). In WT and *Exo1*$^{EK/EK}$ males, spermatogenesis progresses uniformly across the seminiferous epithelium, and mature spermatozoa are released toward the lumen (Fig. 5*E*), indicating full completion of spermatogenesis within these tubules. In contrast to WT and *Exo1*$^{EK/EK}$ mice, the seminiferous tubules of *Exo1*$^{null/null}$ mice were severely depleted of spermatids and spermatozoa (Fig. 5*E*, *Bottom*). However, the presence of pachytene spermatocytes in all three genotypes (Fig. 5*F*) indicates that meiosis can progress through prophase I in *Exo1*$^{null/null}$ mice. *Exo1*$^{null/null}$ mice did display predominantly abnormal metaphase configurations as evidenced by abnormal spindle structures (Fig. 5*G*, *Bottom*), which resulted in spermatocyte apoptosis (Fig. 5*H*).

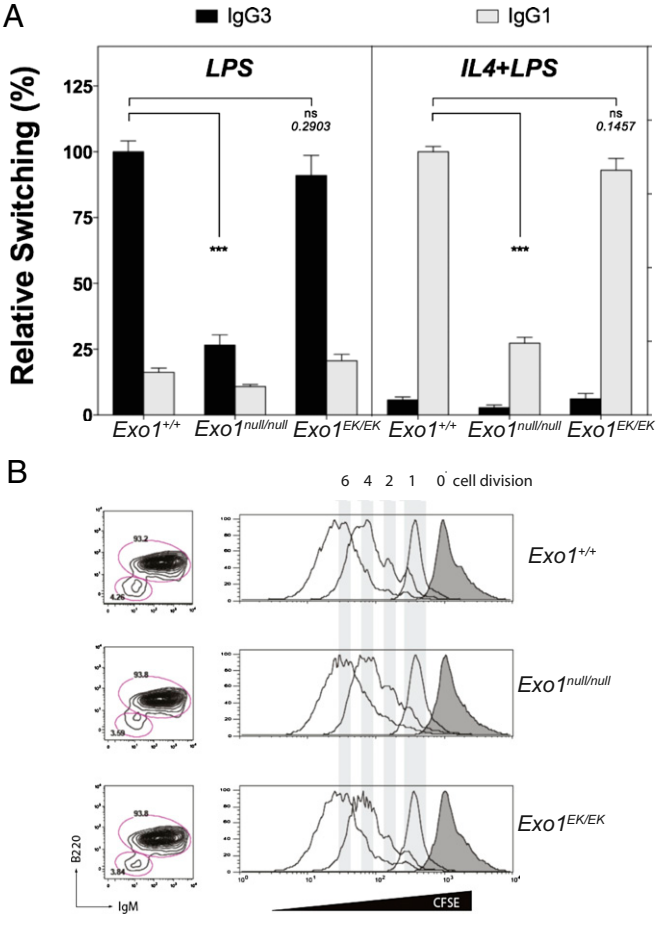

Fig. 4. Reduced ex vivo CSR in *Exo1*$^{null/null}$ mice. (*A*) Relative switching to IgG3 and to IgG1 in a total of four WT, three *Exo1*$^{EK/EK}$ knockin mutant, and three *Exo1*$^{null/null}$ mice. The efficiency of switching in the WT group within each experiment was defined as 100%, and two replicates were assayed for each stimulation (LPS or IL-4+LPS). The data shown represent relative mean efficiency of switching ± SEM. ns, not significant. (*B*) Proliferation of stimulated B cells of the indicated genotypes measured by carboxyfluorescein succinimidyl ester (CFSE) dilution assay. Note that there is no appreciable difference in proliferation. ns, not significant; ***$P < 0.001$.

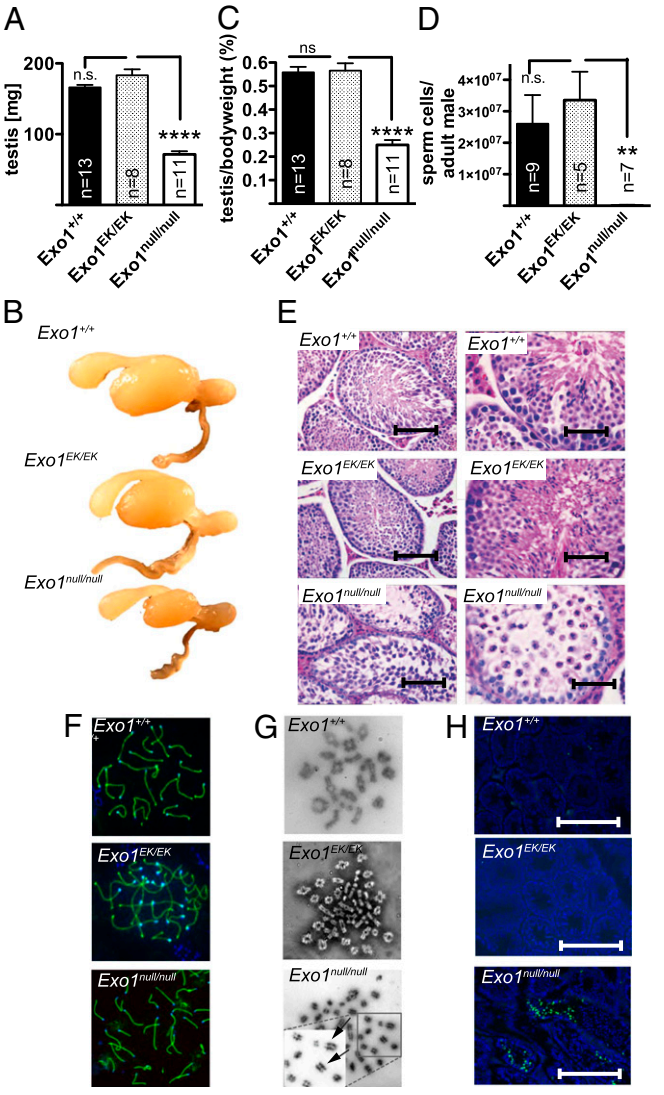

Fig. 5. Exonuclease activity is not required for meiosis. (*A*) Comparison of testis weight of 10-wk-old *Exo1*$^{EK/EK}$, *Exo1*$^{null/null}$, and WT control littermates. (*B*) Comparison of testis size in 10-wk-old *Exo1*$^{EK/EK}$ ($n = 8$), *Exo1*$^{null/null}$ ($n = 11$), and WT control ($n = 13$) littermates. (*C*) Comparison of body weight of 10-wk-old *Exo1*$^{EK/EK}$, *Exo1*$^{null/null}$, and WT control littermates. (*D*) Epididymal sperm counts of 10-wk-old *Exo1*$^{EK/EK}$, *Exo1*$^{null/null}$, and WT control littermates. Note that *Exo1*$^{null/null}$ adult males show a significant decrease in sperm count. Data present mean ± SEM. (*E*) H&E staining of testis sections from WT, *Exo1*$^{EK/EK}$, and *Exo1*$^{null/null}$ mice shown at two different magnifications. (*Left*: magnification: 200×, scale bars, 20 μm; *Right*: magnification: 400×, scale bars, 10 μm). (*F*) Examples of pachytene chromosome configurations after SYCP3 staining of the indicated genotypes, indicating normal progression through prophase I. (*G*) Representative images of metaphase spreads of *Exo1*$^{EK/EK}$, *Exo1*$^{null/null}$, and WT control littermates. (Magnification: 1,000×.) Note that the *Exo1*$^{null/null}$ mice displayed predominantly abnormal spindle structures, with mostly achiasmatic univalent chromosomes. (*Inset*) Twofold magnification of the boxed field of *Exo1*$^{null/null}$ displaying mostly univalent chromosomes (arrows). (*H*) TUNEL staining to detect apoptotic cells (green) in *Exo1*$^{EK/EK}$, *Exo1*$^{null/null}$, and WT-control littermates. Note that the *Exo1*$^{null/null}$ tubules show increased apoptotic cells compared with *Exo1*$^{EK/EK}$ and WT littermates. (Scale bars: 100 μm.) A minimum of 25 images per genotype was analyzed. n.s., not significant; **$P < 0.01$; ****$P < 0.0001$.

Loss of EXO1 or Its Exonuclease Activity Has Distinct Effects on Survival and Tumor Phenotype. Long-term effects of EXO1 inactivation/deletion on survival and cancer susceptibility were studied by following cohorts of $Exo1^{EK/EK}$, $Exo1^{+/EK}$, $Exo1^{null/null}$, $Exo1^{+/null}$, and WT mice over a period of 20 mo. $Exo1^{+/EK}$ and $Exo1^{+/null}$ heterozygote mice did not show reduced survival or increased cancer predisposition. However, $Exo1^{null/null}$ and $Exo1^{EK/EK}$ mice showed significantly reduced survival and accelerated tumorigenesis compared with age-matched WT mice (Fig. 6*A*). Interestingly, although $Exo1^{null/null}$ mice predominantly developed lymphomas, $Exo1^{EK/EK}$ mutant mice showed a significant shift in the tumor spectrum toward sarcomas and adenomas (P = 0.0044) (Fig. 6 *B* and *C*). Using four different markers (A27, D7M91, U12335, and A33), we did not detect microsatellite instability (MSI) in the tumors of either the $Exo1^{EK}$ (0/7) or the $Exo1^{null}$ (0/13) mutant mouse lines, indicating that MSI is not associated with EXO1-dependent tumorigenesis.

The way in which EXO1 is involved in the signaling cascade that leads to the activation of protein 53 (p53) remains unknown. To dissect further the roles of EXO1 in genomic instability and tumor development, we intercrossed the $Exo1^{EK}$ and $Exo1^{null}$ mice with transformation-related protein 53 (*Trp53*) mice to obtain homozygous double-mutant mice. The survival and tumor spectrum of mice of the three different genotypes were analyzed (Fig. 6 *D* and *E*). Interestingly, the survival of $p53^{-/-}$-$Exo1^{EK/EK}$ double-mutant mice was similar to that of $p53^{-/-}$-$Exo1^{+/+}$ single-mutant mice, although the occurrence of sarcomas was increased, and the occurrence of lymphomas was reduced (P = 0.028). In contrast, the survival of $p53^{-/-}$-$Exo1^{null/null}$ mice was reduced significantly in comparison with that of $p53^{-/-}$-$Exo1^{+/+}$ animals, but the tumor spectrum remained unchanged. To investigate the molecular mechanism underlying tumorigenesis in all three cohorts, we analyzed genome-wide genetic instability in the tumors (three tumors per genotype) by array Comparative Genomic Hybridization (aCGH). Interestingly, the $p53^{-/-}$-$Exo1^{null/null}$ tumors showed less segmental chromosomal instability than $p53^{-/-}$-$Exo1^{EK/EK}$ or $p53^{-/-}$-$Exo1^{+/+}$ tumors (Fig. 6*F*).

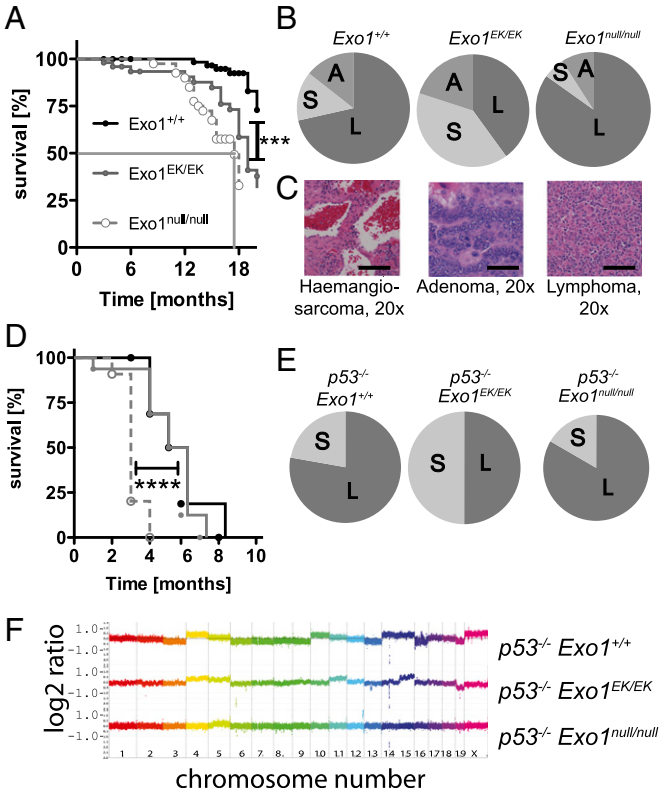

Fig. 6. EXO1 mutation attenuates survival and alters tumor spectrum. The Kaplan–Meier survival curves were generated using the Prism (GraphPad Prism 4.0a) software package. (*A*) The differences between the $Exo1^{EK/EK}$ (n = 50) and $Exo1^{null/null}$ (n = 40) mice are not significant at age 18 mo, but both mouse lines showed a significantly reduced survival as compared with WT littermates (***P < 0.001) (n = 76). The light gray line indicates 50% survival of the $Exo1^{null/null}$ cohort. (*B*) Comparison of tumor spectra in $Exo1^{EK/EK}$ mice (46% of the mice were analyzed with tumors at the age of 18 mo), $Exo1^{null/null}$ mice (80% of the mice were analyzed with tumors at the age of 17 mo), and WT littermates (24% of the mice were analyzed with tumors at the age of 22 mo). Note that the $Exo1^{EK}$ mutation causes a significant shift in tumor spectrum toward sarcoma (S) and adenoma (A) as compared with $Exo1^{null}$ mice (P = 0.0044). L, lymphoma. (*C*) Representative photographs of tumors found in $Exo1^{EK/EK}$ mutant mice. A minimum of 25 images per genotype was analyzed. (Magnification: 200×; scale bars: 500 μm.) (*D*) Survival curve of $p53^{-/-}$-$Exo1^{EK/EK}$ (grey line, n = 16) and $p53^{-/-}$-$Exo1^{null/null}$ (grey dotted line, n = 11) mice compared with $p53^{-/-}$ (black line, n = 18) mice. Note that survival is reduced significantly in $p53^{-/-}$-$Exo1^{null/null}$ mice (****P < 0.0001). (*E*) Comparison of tumor incidence and type in $p53^{-/-}$-$Exo1^{EK/EK}$, $p53^{-/-}$-$Exo1^{null/null}$, and $p53^{-/-}$ mice. (*F*) Representative aCGH analysis of tumors with the indicated *p53-Exo1* genotypes (n = 3 tumors per genotype). Note that the $p53^{-/-}$-$Exo1^{null/null}$ tumors displayed fewer segmental aberrations than the $p53^{-/-}$-$Exo1^{+/+}$ and $p53^{-/-}$-$Exo1^{EK/EK}$ tumors.

Discussion

E109K Mutation Abrogates Exo1 Nuclease Activity. The *EXO1-E109K* mutation was identified in a human patient with atypical HNPCC (25). Subsequent biochemical analysis indicated that the E109K mutation caused the complete inactivation of the exonuclease function (or catalytic activity), but it did not affect protein stability or the ability of the mutant protein to interact with DNA and other MMR proteins (30). As in humans (30), the E109K mutant protein was stably expressed in mice and exhibited impaired enzymatic activity in vitro on nicked DNA substrates (Fig. S2 *A* and *B* and Table S1). We also found that the E109K mutation impaired the nuclease activity on blunt-end substrates (Fig. S2 *C* and *D* and Table S1), similar to the effect reported for the *exo1-D173A* mutation in yeast, which is considered the prototypical Exo1 nuclease-deficient strain (20, 31). Therefore, we conclude that the E109K mutation in mouse *Exo1* reduces its exonuclease activity to below biologically significant levels. This notion is supported further by our finding that both $Exo1^{EK/EK}$ mice and the completely null mice are defective in the formation of ssDNA gaps and DSBs during the DDR to MNNG (Fig. 2 *B*, *C*, and *D*) and also are defective in repairing DSBs and are prone to acquiring chromosomal rearrangements (Fig. 3) and developing tumors (Fig. 6).

Structural Function of EXO1 Is Required for in Vivo MMR. The tissues of $Exo1^{EK/EK}$ mice did not display any increase in mutation frequencies (Fig. 2*A*), thus demonstrating that the exonuclease activity of EXO1 is dispensable for MMR in vivo (Fig. 7). This finding is surprising, because EXO1 remains the only known eukaryotic exonuclease in MMR, and efforts to identify other potential MMR exonucleases in yeast have not succeeded (18). However, these studies have indicated EXO1-independent mechanisms in eukaryotic MMR. Interestingly, loss of Exo1 leads to an accumulation of Mlh1–Pms1 foci (Mlh1–Pms2 or MutLα in mammals) suggesting either that Mlh1–Pms1 complexes may not turn over or that they may play a role in Exo1-independent repair (14). In addition, biochemical studies of human MMR suggest an alternate mechanism of mismatch excision that depends on DNA synthesis-driven strand displacement and the endonuclease function of MutLα (44). In support of this idea, we have shown recently that the PMS2 endonuclease activity is critical for CSR (45), suggesting that PMS2 nuclease could compensate for EXO1 during CSR. However, because PMS2 is not involved in SHM, that rationale does not apply here. Instead, mismatch removal could depend either on other unknown

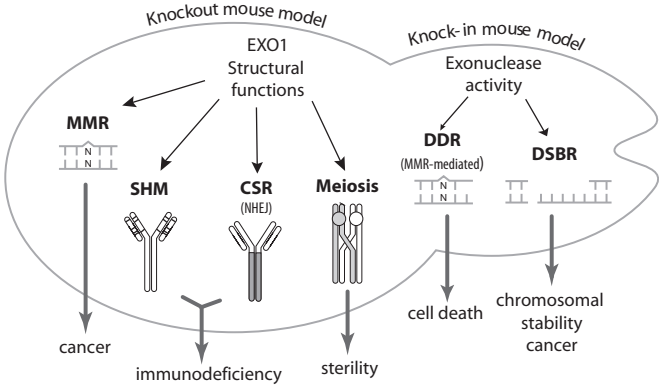

Fig. 7. Model depicting the role of EXO1 in various biological pathways. The structural function of EXO1 is essential for MMR, SHM, CSR, and meiosis, but the exonuclease function of EXO1 is indispensable for ssDNA formation in response to MMR-mediated DDR and DSBR, chromosomal stability, and tumor suppression.

nuclease activities or on the displacement of the mismatched DNA strand by DNA polymerase δ flap activities (44).

Genetic screens in budding yeast previously suggested a role for EXO1 in the formation of larger multiprotein MMR complexes (18), specifically for the stabilization of the MLH1–PMS2 heterodimer (19). Our data, therefore, are consistent with the hypothesis that EXO1 has a structural function in MMR, because the absence of the EXO1 protein in $Exo1^{null/null}$ cell extracts and in mice significantly impairs MMR in vitro and in vivo (Fig. 7). Our data also suggest that $Exo1^{EK/EK}$ mutant cells are MMR proficient because of the presence of the mutant $EXO1^{EK}$ protein that still is able to interact with other MMR proteins such as the MutSα and MutLα heterodimers (30). In addition to EXO1, the MutLα interactome study identified another 5′–3′ exonuclease, Fanconi anemia group D2 protein (FANCD2)-associated nuclease 1 (FAN1) (46–48). Although this notion remains speculative, it is conceivable that during MMR EXO1 might act as a structural noncatalytic adapter for another 5′–3′ exonuclease, such as FAN1, and for other MMR factors, whereas in DSBR, EXO1 catalytic activity might be necessary and sufficient. In fact, this type of structural cooperation has been shown for structure-specific nucleases such as XPF, MUS81, and SLX1, which require adapter partners such as ERCC1, EME1, and SLX4, respectively (49).

EXO1 Nuclease Activity Facilitates the Formation of ssDNA Gaps During DDR. Our studies showed that EXO1 plays a role in the cellular response to MNNG exposure. Loss of either EXO1 protein or the EXO1 nuclease function led to increased MNNG resistance in $Exo1^{null/null}$ or $Exo1^{EK/EK}$ MEFs, respectively (Fig. 2*B*). The increase in MNNG resistance was moderate compared with that in $Exo1^{+/+}$ cells, indicating that alternative enzymes and pathways can partially compensate for the loss of EXO1 function in the process. It is possible that, as in MMR of replication errors, other nucleases or mechanisms participate in the process (44). Interestingly, we found the phosphorylation of RPA and γH2AX after MNNG exposure was reduced in both $Exo1^{null/null}$ and $Exo1^{EK/EK}$ MEFs compared with WT cells (Fig. 2 *C* and *D*). This finding is consistent with the idea that the Exo1 nuclease activity facilitates the formation of ssDNA gaps and DSBs during repeated futile cycles. However, it also is possible that the scaffold function of EXO1 could participate in the direct signaling of DNA damage through its physical interaction with MutSα and MutLα. Although we were not able to observe such a role for EXO1 at physiological levels, the ectopic expression of a human nuclease dead EXO1 construct in mouse EXO1 knockdown MEFs restored the interaction of MSH2 with checkpoint kinase 1 (CHK1) and MNNG sensitivity (50).

EXO1 Nuclease Activity Is Required for the Repair of DNA DSBs Through DNA End Resection. Consistent with previous studies in yeast and eukaryotic cells that suggest a role for EXO1 in DSBR (7, 51–53), both *Exo1*-mutant MEF lines showed reduced colocalization of activated pRPA-S4/S8 with γH2AX without affecting the formation of DSB per se (Fig. 3*C*), indicating that the exonuclease function is indispensable for DSB resection (Fig. 7). In agreement with our findings, previous reports using *exo1*-null and nuclease-deficient yeast strains described increased sensitivity to radiomimetic compounds in both strains, indicating impaired DSBR (31). In addition, DNA end resection processes in yeast appear to be dependent on the nuclease and helicase activities of Exo1, Meiotic recombination 11 homolog 1 (Mre11), and Small growth suppressor 1 (Sgs1) (BLM in humans), respectively (7, 54).

Biochemical studies of human DSBR suggest the existence of two distinct protein complexes in DSBR, one of which requires the enzymatic function of EXO1 in DNA end resection (55). Our results demonstrate that the exonucleolytic activity of EXO1 is of significant importance for maintaining chromosomal stability in mammalian cells because $Exo1^{EK/EK}$ MEFs showed an increased level of chromosomal aberrations similar to those in the $Exo1^{null/null}$ cell lines. In addition, after treatment by a radiomimetic drug, both mutant lines had equally compromised survival as compared with WT cells, thus highlighting the importance of the enzymatic activity of EXO1 for maintaining chromosomal stability, particularly against spontaneously generated DSBs or after low doses of radiomimetic treatments (Fig. 3).

During CSR, S-region DNA DSBs need to be joined by NHEJ factors. Previous studies have shown that MMR proteins are critical for CSR and are important for generating blunt dsDNA breaks in S-regions (8, 41, 42). $Exo1^{null/null}$ mice show deficiencies in SHM and CSR similar to those seen in $Msh2^{-/-}$ mice (56). However, the $Exo1^{EK/EK}$ knockin mutant mice did not show impaired CSR or A:T base mutations in SHM (Fig. 7), indicating that, as in mitotic MMR and meiotic recombination, the structural function of EXO1 is more important than its enzymatic activity in this process (Figs. 2 and 4). V(D)J recombination and CSR are two physiological DSBR systems, recognized and repaired via NHEJ, and neither requires the long stretches of ssDNA seen during HR. However, CSR has been shown to depend on short ssDNA microhomologies, possibly mediated by CtIP resection of DNA ends in a B-cell line (43), although clear evidence for this effect in CtIP-depleted primary B cells is lacking (57). Although CtIP and EXO1 collaborate in the generation of long ssDNA stretches during DSBR, this activity might be uncoupled during CSR. CSR-related NHEJ involves the resection of short end stretches (typically <10 bp) (42), possibly explaining the lack of requirement for EXO1 in regulating NHEJ during CSR. Therefore, the enzymatic activity of EXO1 might be too robust for this repair pathway, and the structural function of the protein might be more important for the correct assembly of higher-order protein complexes involved in CSR. Interestingly, recent studies in mice revealed an important structural role of another repair protein, Rev1, in CSR in the stabilization and/or recruitment of UNG that is independent of the enzymatic function of Rev1 (58).

Structural Function of EXO1 Is Important for Meiosis. In agreement with previous data demonstrating an essential role for EXO1 in meiosis (4, 53, 59), $Exo1^{null/null}$ mice are sterile, resembling the meiotic phenotype observed in $Mlh1^{-/-}$ and $Mlh3^{-/-}$ mice (60, 61). However, surprisingly, EXO1 exonuclease function is dispensable for meiosis in mice (Figs. 5 and 7). Previously, the analysis of MLH1 and MLH3 foci in Exo1-deficient mice

suggested that EXO1 stabilizes the MLH1–MLH3 complexes and implicated EXO1 in the stabilization of crossover events after the accumulation of MLH1 and MLH3 foci (62). Consistent with a stabilizing role for EXO1, studies in yeast recently have uncovered temporally distinct nuclease-dependent and -independent roles for Exo1 during meiosis. Although Exo1 exonuclease activity appears to be required for 5′–3′ end resection following Spo11-induced DSB formation, it seems dispensable for the resolution of crossover-designated intermediates. In the latter case, the physical interaction between EXO1 and the MLH1–MLH3 complex plays a crucial role (20, 63). Accordingly, it is possible that, much as the MLH1–PMS2 nuclease could compensate for loss of EXO1 catalytic activity during CSR, MLH1–MLH3 nuclease could compensate for loss of EXO1 catalytic activity during meiosis in mammals. Furthermore, we have shown recently that the endonuclease function of PMS2 does not play a major role in meiosis (45); this finding hints that different MutL nuclease complexes could have evolved to accomplish distinct nonredundant catalytic functions. Incidentally, *mlh3* nuclease mutants manifest meiotic crossover defects in yeast (64).

Abrogation of the Nuclease Activity of EXO1 Affects Mouse Survival and Tumor Latency. $Exo1^{null/null}$ mice showed reduced survival, which was caused mainly by susceptibility to cancer. Although the $Exo1^{EK/EK}$ mutant mice also had reduced survival, the tumor spectrum was significantly altered compared with $Exo1^{null/null}$ mice (Fig. 6*B*). As expected from our analyses of the mutational frequencies in genomic DNA of mouse tissues in $Exo1^{null/null}$ and $Exo1^{EK/EK}$ mice (Table 1 and Fig. 2*A*), the tumors in both *EXO1*-mutant mice did not display MSI at mono- or dinucleotide repeat markers, unlike tumors from mouse lines with mutations in other MMR genes (65). Although tumorigenesis in $Exo1^{EK/EK}$ mice appears to be caused mainly by the defect in DSBR resulting in increased chromosomal breaks, tumorigenesis in $Exo1^{null/null}$ mice is likely caused by the defects in both DSBR and MMR. Consistent with this notion, we observed not only increased chromosomal breaks in the $Exo1^{null/null}$ cells (Fig. 3*A*) but also an increase in the frequency of base substitution mutations in $Exo1^{null/null}$ mice (Table 1 and Fig. 2*A*).

The different effects of the *Exo1-E109K* and *Exo1-null* mutations on tumorigenesis also were observed in *p53*-deficient mice. Previous analysis of $p53^{-/-}$-$Msh2^{-/-}$ and $p53^{-/-}$-$Msh6^{-/-}$ mice demonstrated that MMR deficiency greatly accelerates p53-driven tumorigenesis, and the mice succumb to early-onset lymphomas (66, 67). In agreement with previous studies (68), the $p53^{-/-}$ mice predominantly developed lymphomas and, to a lesser extent, sarcomas. This tumor spectrum did not change in the $p53^{-/-}$-$Exo1^{null/null}$ mice (Fig. 6*E*); however, $p53^{-/-}$-$Exo1^{null/null}$ mice showed a significantly reduced survival compared with $p53^{-/-}$ mice (Fig. 6*D*). In contrast, the loss of the enzymatic activity did not further affect the survival of $p53^{-/-}$-$Exo1^{EK/EK}$ animals, but it significantly altered the tumor spectrum compared with $p53^{-/-}$ single- or $p53^{-/-}$-$Exo1^{null/null}$ double-mutant mice ($P = 0.02$) (Fig. 6*E*). It is possible that the increase in chromosomal instability caused by the defect in the exonuclease activity of EXO1 underlies the change in the tumor spectrum. Interestingly, sarcoma development is associated with increased chromosomal instability (69), and the defect in DSBR in the $Exo1^{EK}$ mutant mice might contribute to this process in *p53* mutant mice. The reduced survival in the $p53^{-/-}$-$Exo1^{null/null}$ mice likely results from a combination of MMR deficiency (Fig. 2) and impaired DSBR (Fig. 3). However, the relative contributions of the two repair pathways to tumor development in $p53^{-/-}$-$Exo1^{null/null}$ mice cannot be determined completely. Nevertheless, as in other MMR-deficient *p53* mutant mice, the loss of MMR function in $p53^{-/-}$-$Exo1^{null/null}$ mice plays a major role in p53-depedendent lymphomagenesis.

This notion also is supported by the aCGH analysis of tumor DNA in the *p53-Exo1*–mutant mice. In agreement with previous studies in mice and humans (69, 70), the $p53^{-/-}$ tumors showed an increased level of genomic instability (Fig. 6*F*). Strikingly, the tumors in $p53^{-/-}$-$Exo1^{null/null}$ mice contained fewer segmental gains and losses than did $p53^{-/-}$-$Exo1^{EK/EK}$ and $p53^{-/-}$-$Exo1^{+/+}$ tumors. This finding supports the idea that tumorigenesis in $p53^{-/-}$-$Exo1^{null/null}$ animals is driven by an increase in genomic base substitution mutations caused by loss of the structural function and MMR deficiency rather than by an increase in chromosomal instability that is associated with loss of the exonuclease function. In contrast, the defect in DSBR that is caused by loss of the exonuclease function contributes to chromosomal instability and seems to favor the development of sarcomas in $p53^{-/-}$-$Exo1^{EK/EK}$ mice.

Conclusions

In summary, we report that the $Exo1^{EK}$ mutation acts as a separation-of-function mutation demonstrating that EXO1 provides not only an exonuclease but also a structural function and that both EXO1 functions have different implications for DSBR, MMR, meiosis, antibody diversification, and tumor development (Fig. 7). Although EXO1 is essential for all these processes, the exonuclease function of EXO1 is important in the DDR to alkylating agents and is essential for DSBR, chromosomal stability, and tumor suppression. Previous data suggest an important role for EXO1 in human cancer (26). However, direct proof as to whether loss of EXO1 function is causative for cancer development was lacking. The analysis of $Exo1^{null/null}$ and $Exo1^{EK/EK}$ mice indicate that both the structural and exonuclease functions of EXO1 are important in tumor suppression, possibly explaining the atypical nature of some EXO1-associated CRCs. Furthermore, the finding that tumorigenesis can be accelerated or altered in $p53^{-/-}$-$Exo1^{-/-}$ and $p53^{-/-}$-$Exo1^{EK/EK}$ mice, respectively, indicates that EXO1 suppresses tumorigenesis by maintaining genomic stability through its functions in both MMR and DSBR.

Materials and Methods

Antibodies and Western Blot Analysis. Antibodies used were rabbit α-EXO1 (in-house), mouse α-RPA2 (Ab1, 9HD; Lab Vision), rabbit α-RPA pS4/S8 (Bethyl), mouse α-γH2AX (Cell Signaling), mouse α-MSH2 (Ab-2; Calbiochem), ECL anti-rabbit IgG HRP (GE Healthcare), and ECL anti-mouse IgG HRP (GE Healthcare). Nuclear extracts from testes were prepared according to standard protocols (71) and were mixed with equal amounts of Laemmli buffer. Protein was subjected to 7.5% SDS-PAGE and was detected using antibody against mEXO1.

In Vivo Mutation Analysis. The frequency of in vivo mutations in spleen, liver, and small intestine of WT and *Exo1*-mutant mice was assessed using the target *cII* transgene in the Big Blue Transgenic Rodent Mutagenesis Assay System (Stratagene) according to the manufacturer's guidelines (72). Mutation frequency was defined as the ratio of mutant plaques to the total number of plaques screened. To characterize the *cII* locus in mutant phage particles, the entire *cII* gene was PCR amplified and sequenced.

Generation of MEF Strains. MEFs were isolated from embryos at 12.5 or 13.5 d post conception and were maintained according to standard procedures. Each MEF line was expanded to three 10-cm dishes and then was frozen in 90% (vol/vol) FBS, 10% (vol/vol) DMSO and labeled as "passage 1."

MNNG Treatment. Relative cell viability after MNNG treatment was determined using Thiazolyl Blue Tetrazolium Bromide (MTT)-conversion (Sigma). Cells were plated in triplicate in 24-well plates and were allowed to adhere overnight. Cells were pretreated with 20 μM O6-Benzylguanine (O6BG) before the addition of MNNG to inhibit fully the repair of O6meG adducts by O-6-methylguanine-DNA methyltransferase (MGMT). Then 48–72 h after treatment, MTT solution was added to the wells at a final concentration on 0.5 mg/mL, and cells were incubated at 37 °C for an additional 2 h. Medium was removed, and the converted dye was solubilized with acidic iso-

propanol. Absorbance of converted dye was measured at a wavelength of 570 nm using a Perkin Elmer Victor X5 plate reader. Cell viability was calculated relative to DMSO-treated cells incubated in parallel. MNNG and O6BG were purchased from Sigma. Stock solutions were prepared in DMSO and stored at −20 °C until use.

Metaphase Analysis. Metaphase chromosome spreads were prepared following standard procedures. Briefly, after treatment with colcemid (10 ng/mL) for 4 h, cells were harvested, treated with 75 mM KCl for 20 min, and fixed in methanol: acetic acid (3:1) at 25 °C followed by three consecutive washes with methanol: acetic acid (3:1). The cell suspension then was dropped onto a microscope slide and embedded in Vectashield mounting medium for fluorescence with DAPI (Vector) and was analyzed under the fluorescence microscope.

CPT Treatment. Primary MEFs (passage 3) were grown on coverslips and treated with 1 μM CPT or DMSO (control). After 1 h, the drug was removed and cells were pre-extracted for 5 min on ice in 10 mM Pipes buffer (pH 6.8) containing 300 mM sucrose, 50 mM NaCl, 3 mM EDTA, 0.5% Triton X-100, and Protease Inhibitor Mixture (EDTA-free; Roche) before fixation in 2% (wt/vol) paraformaldehyde for 15 min at 25 °C. After fixation, cells were washed with PBS and then were blocked with 5% (wt/vol) BSA and 0.1% Triton X-100 in PBS. Cells were stained with primary antibodies *en bloc* for 1 h, washed in PBS + 0.1% Triton X-100, then stained with Alexa 488 goat anti-mouse/rabbit, and Alexa 598 goat anti-mouse/rabbit (Molecular Probes) for 1 h at 25 °C *en bloc*. DNA was counterstained with DAPI in Vectashield mounting agent (Vector). Images were acquired using a Bio-Rad Radiance 2100 (Nikon Eclipse E800) microscope using Lasersharp 2000 software (Zeiss).

Clonogenic Assay. Immortalized MEFs of all three genotypes ($Exo1^{+/+}$, $Exo1^{EK/EK}$, and $Exo1^{null/null}$) were seeded in single-cell suspensions (500 cells) on six-well plates and 24 h after plating were treated with increasing concentrations (0–10 nM) of CPT or equal amounts of DMSO as control. Medium containing CPT or DMSO was refreshed every 48–72 h until colony growth was detected. Seven days after treatment cells were stained with crystal violet according standard procedure, and cell survival was evaluated by colony counts.

Somatic Hypermutation Analysis. Six-week-old $Exo1^{EK/EK}$, $Exo1^{null/null}$, and WT littermates were immunized i.p. with (4-hydroxy-3-nitrophenyl)acetyl $(NP)_{30}$-CGG (BioSearch Technologies) in alum (Pierce) as in ref. 4 and were boosted 4 wk after primary immunization. Hypermutation analysis was performed as previously described (39).

Ex Vivo Class-Switching Assay. Splenic B cells from immunized and non-immunized $Exo1^{EK/EK}$, $Exo1^{null/null}$, and WT littermates were isolated and depleted of T cells by complement-mediated lysis (73). Splenocytes were stimulated with either 50 μg/mL of LPS (Sigma) or LPS plus 50 ng/mL of recombinant IL-4 (R&D Systems). After 4 d in culture, surface IgM and IgG were stained and analyzed by FACS as previously described (74).

Analysis of Meiotic Prophase I. Chromosome spreads were prepared as described previously (4, with modifications. Further treatment and analysis were carried out as described previously (45).

TUNEL Staining. The rate of apoptosis was determined by TUNEL assay (DeadEnd Fluorometric TUNEL System; Promega) on 5-μm-thick paraffin sections of testis. The number of apoptotic cells per testicle tubule was counted in 20 low-power (200×) fields per mouse (n = 4–5 mice per group).

Analysis of Tumors and Survival. Mice were observed until they became morbid or moribund. Tumors from killed mice were removed and fixed in 10% (vol/vol) neutral buffered formalin. All tumors were processed for paraffin embedding, and sections were prepared for staining with H&E according to standard procedures. Statistical analysis of tumor incidence was performed using the Fisher's exact test. Mutations in microsatellite sequences were assayed by PCR of tumor DNA. Equal amounts of tail and tumor DNA from five mice of each mouse strain ($Exo1^{+/+}$, $Exo1^{EK/EK}$, and $Exo1^{null/null}$) were analyzed by PCR as described previously (4). The Kaplan–Meier method was used to compare curves for survival, with significance evaluated by two-sided log rank.

aCGH. Five to ten micrograms of genomic DNA from frozen primary tumors were analyzed for aCGH using the 3× 720K platform (Roche NimbleGen) according to the manufacturers' protocol. Genomic DNA from tail was used as reference DNA.

Bioinformatics Analysis. Raw microarray intensities were normalized using the variance-stabilizing algorithm (*vs.n*) implemented in Bioconductor package *limma*. Normalized log2 ratios were segmented using three popular algorithms, unsupervised hidden Markov model (HomHMM), circular binary segmentation (DNAcopy), and GLAD, using the Bioconductor package *snapCGH*. We define low-level gain and loss as log2 values of 0.5 and −0.5, respectively, and high-level amplification and deletion as +0.6 and −1 (75–77).

ACKNOWLEDGMENTS. This work was supported by the National Institutes of Health (NIH) Grants CA72649 and CA102705 (to M.D.S.) and CA76329 and CA93484 (to W.E.) and by Project Z01 ES065089 from the Division of Intramural Research of the National Institute of Environmental Health Sciences, NIH (to T.A.K.). R.S.S. is supported by P30CA013330 from the National Cancer Institute. M.D.S. is supported by the Harry Eagle Chair, provided by the National Women's Division of the Albert Einstein College of Medicine. S.S. was supported by Deutsche Forschungsgemeinschaft Grant SCHA 1557/1-1.

1. Szankasi P, Smith GR (1992) A DNA exonuclease induced during meiosis of Schizosaccharomyces pombe. *J Biol Chem* 267(5):3014–3023.
2. Tishkoff DX, et al. (1997) Identification and characterization of Saccharomyces cerevisiae EXO1, a gene encoding an exonuclease that interacts with MSH2. *Proc Natl Acad Sci USA* 94(14):7487–7492.
3. Genschel J, Bazemore LR, Modrich P (2002) Human exonuclease I is required for 5′ and 3′ mismatch repair. *J Biol Chem* 277(15):13302–13311.
4. Wei K, et al. (2003) Inactivation of Exonuclease 1 in mice results in DNA mismatch repair defects, increased cancer susceptibility, and male and female sterility. *Genes Dev* 17(5):603–614.
5. Zhu Z, Chung WH, Shim EY, Lee SE, Ira G (2008) Sgs1 helicase and two nucleases Dna2 and Exo1 resect DNA double-strand break ends. *Cell* 134(6):981–994.
6. Mimitou EP, Symington LS (2008) Sae2, Exo1 and Sgs1 collaborate in DNA double-strand break processing. *Nature* 455(7214):770–774.
7. Gravel S, Chapman JR, Magill C, Jackson SP (2008) DNA helicases Sgs1 and BLM promote DNA double-strand break resection. *Genes Dev* 22(20):2767–2772.
8. Bardwell PD, et al. (2004) Altered somatic hypermutation and reduced class-switch recombination in exonuclease 1-mutant mice. *Nat Immunol* 5(2):224–229.
9. Vallur AC, Maizels N (2010) Distinct activities of exonuclease 1 and flap endonuclease 1 at telomeric g4 DNA. *PLoS ONE* 5(1):e8908.
10. Lee BI, Wilson DM, 3rd (1999) The RAD2 domain of human exonuclease 1 exhibits 5′ to 3′ exonuclease and flap structure-specific endonuclease activities. *J Biol Chem* 274(53):37763–37769.
11. Orans J, et al. (2011) Structures of human exonuclease 1 DNA complexes suggest a unified mechanism for nuclease family. *Cell* 145(2):212–223.
12. Modrich P (2006) Mechanisms in eukaryotic mismatch repair. *J Biol Chem* 281(41): 30305–30309.
13. Mendillo ML, et al. (2010) Probing DNA- and ATP-mediated conformational changes in the MutS family of mispair recognition proteins using deuterium exchange mass spectrometry. *J Biol Chem* 285(17):13170–13182.
14. Hombauer H, Campbell CS, Smith CE, Desai A, Kolodner RD (2011) Visualization of eukaryotic DNA mismatch repair reveals distinct recognition and repair intermediates. *Cell* 147(5):1040–1053.
15. Flores-Rozas H, Kolodner RD (1998) The Saccharomyces cerevisiae MLH3 gene functions in MSH3-dependent suppression of frameshift mutations. *Proc Natl Acad Sci USA* 95(21):12404–12409.
16. Chen PC, et al. (2005) Contributions by MutL homologues Mlh3 and Pms2 to DNA mismatch repair and tumor suppression in the mouse. *Cancer Res* 65(19):8662–8670.
17. Schmutte C, et al. (1998) Human exonuclease I interacts with the mismatch repair protein hMSH2. *Cancer Res* 58(20):4537–4542.
18. Amin NS, Nguyen MN, Oh S, Kolodner RD (2001) exo1-Dependent mutator mutations: Model system for studying functional interactions in mismatch repair. *Mol Cell Biol* 21(15):5142–5155.
19. Tran PT, et al. (2007) A mutation in EXO1 defines separable roles in DNA mismatch repair and post-replication repair. *DNA Repair (Amst)* 6(11):1572–1583.
20. Keelagher RE, Cotton VE, Goldman AS, Borts RH (2011) Separable roles for Exonuclease I in meiotic DNA double-strand break repair. *DNA Repair (Amst)* 10(2):126–137.
21. Peled JU, et al. (2008) The biochemistry of somatic hypermutation. *Annu Rev Immunol* 26:481–511.
22. Kolodner RD, et al. (1995) Structure of the human MLH1 locus and analysis of a large hereditary nonpolyposis colorectal carcinoma kindred for mlh1 mutations. *Cancer Res* 55(2):242–248.
23. Peltomäki P (2003) Role of DNA mismatch repair defects in the pathogenesis of human cancer. *J Clin Oncol* 21(6):1174–1179.
24. Mueller J, et al. (2009) Comprehensive molecular analysis of mismatch repair gene defects in suspected Lynch syndrome (hereditary nonpolyposis colorectal cancer) cases. *Cancer Res* 69(17):7053–7061.
25. Wu Y, et al. (2001) Germline mutations of EXO1 gene in patients with hereditary nonpolyposis colorectal cancer (HNPCC) and atypical HNPCC forms. *Gastroenterology* 120(7):1580–1587.

26. Liberti SE, Rasmussen LJ (2004) Is hEXO1 a cancer predisposing gene? *Mol Cancer Res* 2(8):427–432.
27. Nimonkar AV, Ozsoy AZ, Genschel J, Modrich P, Kowalczykowski SC (2008) Human exonuclease 1 and BLM helicase interact to resect DNA and initiate DNA repair. *Proc Natl Acad Sci USA* 105(44):16906–16911.
28. Hartlerode AJ, Scully R (2009) Mechanisms of double-strand break repair in somatic mammalian cells. *Biochem J* 423(2):157–168.
29. Mimitou EP, Symington LS (2009) DNA end resection: Many nucleases make light work. *DNA Repair (Amst)* 8(9):983–995.
30. Sun X, Zheng L, Shen B (2002) Functional alterations of human exonuclease 1 mutants identified in atypical hereditary nonpolyposis colorectal cancer syndrome. *Cancer Res* 62(21):6026–6030.
31. Tran PT, Erdeniz N, Dudley S, Liskay RM (2002) Characterization of nuclease-dependent functions of Exo1p in Saccharomyces cerevisiae. *DNA Repair (Amst)* 1(11): 895–912.
32. Iyer RR, Pluciennik A, Burdett V, Modrich PL (2006) DNA mismatch repair: Functions and mechanisms. *Chem Rev* 106(2):302–323.
33. Stojic L, Brun R, Jiricny J (2004) Mismatch repair and DNA damage signalling. *DNA Repair (Amst)* 3(8-9):1091–1101.
34. Fishel R (2001) The selection for mismatch repair defects in hereditary nonpolyposis colorectal cancer: Revising the mutator hypothesis. *Cancer Res* 61(20):7369–7374.
35. Karran P (2001) Mechanisms of tolerance to DNA damaging therapeutic drugs. *Carcinogenesis* 22(12):1931–1937.
36. Kat A, et al. (1993) An alkylation-tolerant, mutator human cell line is deficient in strand-specific mismatch repair. *Proc Natl Acad Sci USA* 90(14):6424–6428.
37. Wang H, Hays JB (2006) Construction of MMR plasmid substrates and analysis of MMR error correction and excision. *Methods Mol Biol* 314:345–353.
38. Faili A, et al. (2004) DNA polymerase eta is involved in hypermutation occurring during immunoglobulin class switch recombination. *J Exp Med* 199(2):265–270.
39. Roa S, et al. (2010) MSH2/MSH6 complex promotes error-free repair of AID-induced dU:G mispairs as well as error-prone hypermutation of A:T sites. *PLoS ONE* 5(6): e11182.
40. Jackson SP, Bartek J (2009) The DNA-damage response in human biology and disease. *Nature* 461(7267):1071–1078.
41. Maul RW, Gearhart PJ (2010) AID and somatic hypermutation. *Adv Immunol* 105: 159–191.
42. Stavnezer J, Björkman A, Du L, Cagigi A, Pan-Hammarström Q (2010) Mapping of switch recombination junctions, a tool for studying DNA repair pathways during immunoglobulin class switching. *Adv Immunol* 108:45–109.
43. Lee-Theilen M, Matthews AJ, Kelly D, Zheng S, Chaudhuri J (2011) CtIP promotes microhomology-mediated alternative end joining during class-switch recombination. *Nat Struct Mol Biol* 18(1):75–79.
44. Kadyrov FA, et al. (2009) A possible mechanism for exonuclease 1-independent eukaryotic mismatch repair. *Proc Natl Acad Sci USA* 106(21):8495–8500.
45. van Oers JM, et al. (2010) PMS2 endonuclease activity has distinct biological functions and is essential for genome maintenance. *Proc Natl Acad Sci USA* 107(30): 13384–13389.
46. Cannavo E, Gerrits B, Marra G, Schlapbach R, Jiricny J (2007) Characterization of the interactome of the human MutL homologues MLH1, PMS1, and PMS2. *J Biol Chem* 282(5):2976–2986.
47. Kratz K, et al. (2010) Deficiency of FANCD2-associated nuclease KIAA1018/FAN1 sensitizes cells to interstrand crosslinking agents. *Cell* 142(1):77–88.
48. Smogorzewska A, et al. (2010) A genetic screen identifies FAN1, a Fanconi anemia-associated nuclease necessary for DNA interstrand crosslink repair. *Mol Cell* 39(1): 36–47.
49. Ciccia A, McDonald N, West SC (2008) Structural and functional relationships of the XPF/MUS81 family of proteins. *Annu Rev Biochem* 77:259–287.
50. Izumchenko E, Saydi J, Brown KD (2012) Exonuclease 1 (Exo1) is required for activating response to S(N)1 DNA methylating agents. *DNA Repair (Amst)* 11(12):951–64.
51. Schaetzlein S, et al. (2007) Exonuclease-1 deletion impairs DNA damage signaling and prolongs lifespan of telomere-dysfunctional mice. *Cell* 130(5):863–877.
52. Moreau S, Morgan EA, Symington LS (2001) Overlapping functions of the Saccharomyces cerevisiae Mre11, Exo1 and Rad27 nucleases in DNA metabolism. *Genetics* 159(4): 1423–1433.
53. Tsubouchi H, Ogawa H (2000) Exo1 roles for repair of DNA double-strand breaks and meiotic crossing over in Saccharomyces cerevisiae. *Mol Biol Cell* 11(7):2221–2233.
54. Garcia V, Phelps SE, Gray S, Neale MJ (2011) Bidirectional resection of DNA double-strand breaks by Mre11 and Exo1. *Nature* 479(7372):241–244.
55. Nimonkar AV, et al. (2011) BLM-DNA2-RPA-MRN and EXO1-BLM-RPA-MRN constitute two DNA end resection machineries for human DNA break repair. *Genes Dev* 25(4): 350–362.
56. Rada C, Ehrenstein MR, Neuberger MS, Milstein C (1998) Hot spot focusing of somatic hypermutation in MSH2-deficient mice suggests two stages of mutational targeting. *Immunity* 9(1):135–141.
57. Bothmer A, et al. (2013) Mechanism of DNA resection during intrachromosomal recombination and immunoglobulin class switching. *J Exp Med* 210(1):115–123.
58. Zan H, et al. (2012) Rev1 recruits Ung to switch regions and enhances dU glycosylation for immunoglobulin class switch DNA recombination. *Cell Rep* 2(5):1220–32.
59. Kirkpatrick DT, Ferguson JR, Petes TD, Symington LS (2000) Decreased meiotic intergenic recombination and increased meiosis I nondisjunction in exo1 mutants of Saccharomyces cerevisiae. *Genetics* 156(4):1549–1557.
60. Edelmann W, et al. (1996) Meiotic pachytene arrest in MLH1-deficient mice. *Cell* 85(7): 1125–1134.
61. Lipkin SM, et al. (2002) Meiotic arrest and aneuploidy in MLH3-deficient mice. *Nat Genet* 31(4):385–390.
62. Kan R, et al. (2008) Comparative analysis of meiotic progression in female mice bearing mutations in genes of the DNA mismatch repair pathway. *Biol Reprod* 78(3): 462–471.
63. Zakharyevich K, et al. (2010) Temporally and biochemically distinct activities of Exo1 during meiosis: Double-strand break resection and resolution of double Holliday junctions. *Mol Cell* 40(6):1001–1015.
64. Nishant KT, Plys AJ, Alani E (2008) A mutation in the putative MLH3 endonuclease domain confers a defect in both mismatch repair and meiosis in Saccharomyces cerevisiae. *Genetics* 179(2):747–755.
65. Taketo MM, Edelmann W (2009) Mouse models of colon cancer. *Gastroenterology* 136(3):780–798.
66. Cranston A, et al. (1997) Female embryonic lethality in mice nullizygous for both Msh2 and p53. *Nat Genet* 17(1):114–118.
67. Young LC, et al. (2007) The associated contributions of p53 and the DNA mismatch repair protein Msh6 to spontaneous tumorigenesis. *Carcinogenesis* 28(10):2131–2138.
68. Jacks T, et al. (1994) Tumor spectrum analysis in p53-mutant mice. *Curr Biol* 4(1):1–7.
69. Overholtzer M, et al. (2003) The presence of p53 mutations in human osteosarcomas correlates with high levels of genomic instability. *Proc Natl Acad Sci USA* 100(20): 11547–11552.
70. Fukasawa K, Wiener F, Vande Woude GF, Mai S (1997) Genomic instability and apoptosis are frequent in p53 deficient young mice. *Oncogene* 15(11):1295–1302.
71. Dignam JD, Lebovitz RM, Roeder RG (1983) Accurate transcription initiation by RNA polymerase II in a soluble extract from isolated mammalian nuclei. *Nucleic Acids Res* 11(5):1475–1489.
72. Dycaico MJ, et al. (1994) The use of shuttle vectors for mutation analysis in transgenic mice and rats. *Mutat Res* 307(2):461–478.
73. Schrader CE, Edelmann W, Kucherlapati R, Stavnezer J (1999) Reduced isotype switching in splenic B cells from mice deficient in mismatch repair enzymes. *J Exp Med* 190(3):323–330.
74. Li Z, et al. (2006) A role for Mlh3 in somatic hypermutation. *DNA Repair (Amst)* 5(6): 675–682.
75. Nakao K, et al. (2004) High-resolution analysis of DNA copy number alterations in colorectal cancer by array-based comparative genomic hybridization. *Carcinogenesis* 25(8):1345–1357.
76. Hupé P, Stransky N, Thiery JP, Radvanyi F, Barillot E (2004) Analysis of array CGH data: From signal ratio to gain and loss of DNA regions. *Bioinformatics* 20(18):3413–3422.
77. Olshen AB, Venkatraman ES, Lucito R, Wigler M (2004) Circular binary segmentation for the analysis of array-based DNA copy number data. *Biostatistics* 5(4):557–572.